Wu Tong (Orcid ID: 0000-0002-0705-3768)
Fu Suiyan (Orcid ID: 0000-0002-3858-1555)
Xie Lun (Orcid ID: 0000-0003-0783-932X)
Zong Qiu-Gang (Orcid ID: 0000-0002-6414-3794)
Zhou Xu-Zhi (Orcid ID: 0000-0003-4953-1761)
Yue Chao (Orcid ID: 0000-0001-9720-5210)
Sun Weijie (Orcid ID: 0000-0001-5260-658X)
Pu Zuyin (Orcid ID: 0000-0002-8458-6648)
Xiong Ying (Orcid ID: 0000-0002-6286-3034)
Zhao Shaojie (Orcid ID: 0000-0001-9042-5472)

Cluster Observations on Time-of-Flight Effect of Oxygen Ions in Magnetotail Reconnection Exhaust

T. Wu[1], S. Y. Fu[1], L. Xie[1], Q.-G. Zong[1], X. Z. Zhou[1], C. Yue[1], W. J. Sun[2], Z. Y. Pu[1], Y. Xiong[1], S. J. Zhao[1], H. Zhang[1], and F. B. Yu[1]

[1] School of Earth and Space Sciences, Peking University, Beijing, China.

[2] Department of Climate and Space Sciences and Engineering, University of Michigan, Ann Arbor, MI, USA.

Corresponding author: Suiyan Fu (suiyanfu@pku.edu.cn)

Key Points:

- The Time-of-Flight (ToF) effect of O^+ ions in magnetotail reconnection exhaust was observed by Cluster spacecraft.
- The observed cut-off velocity of O^+ is smaller than that of H^+, indicating that O^+ may have a larger diffusion region than H^+.
- A remote-sensing method to estimate the spatial scale ratio between O^+ and H^+ diffusion regions is introduced.

This is the author manuscript accepted for publication and has undergone full peer review but has not been through the copyediting, typesetting, pagination and proofreading process, which may lead to differences between this version and the Version of Record. Please cite this article as doi: 10.1029/2019GL085200

Abstract

The D-shaped ion velocity distribution generated by the time-of-flight (ToF) effect can be considered as an important characteristic of reconnection exhausts in the magnetopause and magnetotail reconnection processes. In this study, we reported the D-shaped velocity distribution of O^+ ions produced by the ToF effect in the magnetotail reconnection exhaust based on the observations from the Cluster spacecraft. The observed cut-off velocity of O^+ ions is smaller than that of H^+ ions at the same time, which is different from the previous theoretical prediction. We suggested that the difference between the two cut-off velocities is probably due to O^+ ions having a larger reconnection diffusion region than H^+ ions. We also demonstrated a remote-sensing method to estimate the spatial scale ratio between the O^+ and H^+ diffusion regions and the distance from the observation site to the center of the magnetotail reconnection region.

Plain Language Summary

The reconnection processes at the Earth's magnetopause and magnetotail can convert the magnetic energy into the kinetic energy of the plasma, thus producing high-speed reconnection exhausts. The exhausting ions usually show a D-shaped velocity distribution caused by the time-of-flight effect. Previous works usually focused only on exhausting protons from the reconnection site, while O^+ ions could also be abundant during geomagnetic active times. In this study, we analyzed a reconnection event to investigate the behaviors of O^+ and H^+ ions in the magnetotail reconnection exhaust region using the observations from the Cluster spacecraft. It is suggested that different behaviors of H^+ and O^+ ions are probably due to O^+ ions having a larger reconnection diffusion region than H^+ ions. In addition, we proposed a remote-sensing method to estimate the spatial scale ratio between the O^+ and H^+ diffusion regions and the distance from the observation site to the center of the magnetotail reconnection region.

1 Introduction

Magnetotail reconnection is one of the key physical processes in the research field of space physics (Vasyliunas, 1975). Both observation and simulation results have suggested that the core region of magnetotail reconnection is composed of an electron diffusion region embedded in an ion diffusion region. The spatial scale of each diffusion region is comparable to the inertia scale of the corresponding particles (Shay et al., 1998; Eastwood et al., 2010). In the proton diffusion region, protons are demagnetized, but electrons remain frozen-in to the magnetic field. In the electron diffusion region, both protons and electrons are demagnetized. Outside the diffusion area, there are separate inflow and exhaust regions, and the speed of the reconnection exhaust is considered to be approximately equal to the upstream Alfvén speed, whereas the inflow velocity is considerably lower (Sonnerup, 1979). The ions in the exhaust region usually form D-shaped velocity distribution characterized by the existence of a lower velocity boundary in the parallel

direction (Phan et al., 2001). Fuselier et al. (2005) proposed that the D-shaped velocity distribution is the result of the time-of-flight (ToF) effect, which will be discussed in detail in Section 3.

When a large number of O^+ ions populate the magnetopause and magnetotail plasma sheet during disturbed times (Kistler et al., 2005, 2006; Mouikis et al., 2010; Kronberg et al., 2014; Yue et al., 2018, 2019), the reconnection processes are significantly affected by these heavy ions (at the magnetopause: Wang et al., 2015; Fuselier et al., 2017, 2019; at the magnetotail: Karimabadi et al., 2011; Liu et al., 2013). Ruan et al. (2005) reported that O^+ ions can be found in the earthward high-speed flows in the magnetotail, which is believed to be the result of the reconnection involving O^+ ions. Besides, many other phenomena observed in the magnetotail, such as plasmoids (Zong et al., 1997, 2004), flux ropes (Wilken et al., 1995), bursty bulk flows (Zong et al., 2008), dipolarization fronts (Zhao et al., 2018), and energetic O^+ layer (Wu et al., 2016), are also considered to be associated with O^+ ions involved in the reconnection processes.

The numerical simulations are widely used to study the influences of O^+ ions on the reconnection process. Shay and Swisdak (2004) suggested that there exist new scales in the reconnection region with three-species plasma, including O^+ ions, and the speed of the reconnection exhaust can be a factor of 2 slower than that expected based on the reconnection rate with only protons and electrons present. In the three-species particle-in-cell simulation, Liu et al. (2015) showed that O^+ ions become demagnetized earlier during their entry into the reconnection site along with protons and electrons, and form a larger diffusion region outside the H^+ diffusion region. Other O^+ ions-related effects in the reconnection process are also reported in simulation works, such as lowering of the reconnection rate, changes in the spatial structure of quadrupole electric field, and modification in the threshold value of instabilities that trigger the reconnection process (Liu et al., 2014; Liang et al., 2016, 2017; Tenfjord et al., 2019).

In most of the previous simulation works, the mass density of O^+ ions is usually set high, and the temperature is set close to zero in the initial state (Markidis et al., 2011; Tenfjord et al., 2018). However, in the Earth's magnetotail, protons and electrons usually dominate, whereas the number density of O^+ ions is often very low (Kistler et al., 2005). O^+ ions can only enter the magnetosphere when they reach a certain energy level after being accelerated during the ionospheric outflowing process, and the characteristic energy of O^+ ions can be as high as several keVs in the magnetotail plasma sheet (Lennartsson & Shelley, 1986). Therefore, to have a clear understanding of how O^+ ions affect the reconnection process, in-situ observations are required.

In this study, we investigated a magnetotail reconnection event with significant O^+ exhaust using the observations from the Cluster spacecraft. The D-shaped velocity distribution of the exhausting O^+ ions was reported in Section 2. We also found that the cut-off velocity of O^+ ions was smaller than that of H^+ ions at the same time, which could be explained by the existence of a larger O^+ diffusion region. A remote-sensing method to estimate the spatial scale ratio between the diffusion regions and the distance from the spacecraft to the center of the reconnection region was discussed in Section 3.

2 Observation

The data used in this study are obtained from the Cluster mission. The magnetic field measurements are from the fluxgate magnetometer (FGM) instrument (Balogh et al., 2001). The ion data are from the Cluster Ion Spectrometry (CIS) package, time-of-flight ion Composition and Distribution Function analyzer (CODIF) and Hot Ion Analyzer (HIA) instruments (Reme et al., 2001). The electron data are from the Plasma Electron and Current Experiment (PEACE) instrument (Johnstone et al., 1997). The coordinate system used in this study are the geocentric solar magnetospheric (GSM) coordinate system, if not mentioned otherwise.

An overview of the event, including the magnetic field and plasma measurements of Cluster SC1 from 16:22 UT to 16:30 UT on August 17, 2001, during the initial phase of a geomagnetic storm with a minimum Dst index of -105 nT, is shown in Figure 1. The spacecraft was located in the magnetotail at ~[-18.3, -4.88, 0.55] R_E at 16:22 UT. Echer et al. (2008) showed that a large number of O^+ ions (~4.0×10^{24} ions/s) escaped into the magnetotail during the initial phase of this geomagnetic storm.

From 16:22:00 UT to 16:23:20 UT, as shown using a blue bar at the top of Figure 1, the characteristic energies of H^+ and O^+ ions were ~1–10 keV (Figures 1b and 1c). The number density of H^+ ions was ~1.0 cm^{-3} (Figure 1d), and the temperature was ~70 MK (Figure 1e). These observations are consistent with the plasma sheet features. The dominant magnetic field component was in the -X direction (Figure 1a) and the total magnetic field intensity was ~40 nT, indicating that the spacecraft was located in the southern outer part of the central plasma sheet. With the increase in the O^+ and H^+ bulk velocities (Figures 1f and 1g) from ~16:23:20 UT to ~16:27:00 UT, the spacecraft crossed the tailward exhaust of a magnetic reconnection region (red bar at the top of Figure 1). It is observed from the energy spectra of O^+ and H^+ ions (Figures 1b and 1c) that O^+ ions in the exhaust region have higher energies than that in the plasma sheet.

After 16:27 UT (green bar at the top of Figure 1), the X component of the magnetic field showed a further decrease. The number densities of H^+ and O^+ ions decreased to ~0.1 cm^{-3}. Meanwhile, the magnitude of O^+ bulk velocity in the -X direction also decreased from ~300 km/s to ~100 km/s. Figures 1h and 1j show the pitch angle distributions of high-energy (5 keV to 10 keV), middle-energy (0.5 keV to 1.5 keV) and low-energy (5 eV to 200 eV) electrons. The behaviors of electrons observed before and after 16:27 UT were different. Before 16:27 UT, electrons mainly showed bidirectional distribution in the 0.5–1.5 keV energy range (Figure 1i). In contrast, after 16:27 UT, the spacecraft observed low-energy (<200 eV) electrons moving along the magnetic field with their pitch angle less than 90° (Figure 1j). Moreover, the temperatures of O^+ and H^+ ions decreased significantly from ~80 MK to ~10 MK (Figure 1e). These observations suggest that the spacecraft crossed the reconnection separatrix at ~16:27 UT, and then entered the plasma sheet boundary layer (PSBL, Eastman et al., 1984). From ~16:27 UT to ~16:30 UT, two significant tailward H^+ flows with their maximum bulk velocity exceeding 1000 km/s were observed, but there was no corresponding high-speed O^+ flow present, indicating that these H^+ populations might have sources other than the previously-observed reconnection exhaust.

Figure 2 shows the observations of O^+ ions in the reconnection exhaust in detail. Figures 2a and 2b show the parallel and perpendicular bulk velocities of O^+ and H^+ ions between 16:22 UT and 16:28 UT. The parallel velocity of O^+ ions was smaller than that of H^+ ions in the exhaust region, indicating that O^+ ions did not obtain the same bulk velocity as H^+ ions in the reconnection diffusion region during this event, although the perpendicular velocity of O^+ ions was close to that of H^+ ions. Figures 2c and 2d show the parallel and perpendicular energy spectra of O^+ ions. The dashed line in Figure 2d indicates the estimated O^+ characteristic energy based on the ion perpendicular velocity obtained using the HIA instrument, which agrees well with the energy of the maximum perpendicular flux. These results imply that the frozen-in condition was satisfied for O^+ ions in the exhaust region.

It's worth pointing out that various factors may have caused biases in the results of O^+ and H^+ bulk velocities. First, due to the upper energy limit of the CODIF instrument, ions with E > 38 keV were not detected, which might cause the underestimation of O^+ and H^+ bulk velocities. Second, return beams might exist at higher energies in the H^+ distributions and could produce an overall lower H^+ velocity. Third, the high-flux H^+ ions might contaminate the data of O^+ ions, and thus influence the calculation of the O^+ velocity. In addition, the local cold O^+ population (discussed later) might reduce the overall parallel velocity of the O^+ ions.

It's observed that there was a clear ascending lower boundary in the parallel spectrum (Figure 2c) when the spacecraft was located in the exhaust region from ~16:24 UT to ~16:26 UT. Figures 2e to 2m show the velocity distributions of O^+ ions observed by SC1 at three different times marked with black arrows above Figure 2c. Each column corresponds to 16:24:17 UT, 16:25:05 UT, and 16:25:45 UT, respectively (sampling time is 8 s for each plot). The first row shows slices in the v_{par} - v_{perp1} plane and the second row shows slices in the v_{perp1} - v_{perp2} plane, in which v_{perp1} corresponds to the E×B direction and v_{perp2} is perpendicular to v_{par} and v_{perp1}.

It can be seen from Figures 2e–2j that O^+ ions in the exhaust region were composed of two different populations. The high energy O^+ population moving along the v_{par} direction, as shown in Figures 2e–2g, was apparently part of the reconnection exhaust. The other population with lower energy can be clearly seen in Figures 2i and 2j. They were relatively cold and moved exactly along the v_{perp1} direction. We believe that these O^+ ions were pre-existing local O^+ ions in the plasma sheet, and the E×B drift leads to their perpendicular motion, as shown in Figure 2d. Unlike the exhausting O^+ population, this cold population was not always present in the exhaust region (Figure 2d), indicating that there might be temporal changes in the O^+ distribution. It should be noted that the O^+ ions with ~1 keV energy observed around 16:24:30 UT in Figure 2c were part of this cold O^+ population rather than part of the reconnection exhaust.

Figures 2k–2m show the integrated v_{par} - v_{perp} O^+ velocity distributions in the bulk v_{perp} = 0 reference frame (resampling grid size is 50 km/s). As can be seen, the distributions of exhausting O^+ ions have D-shaped signatures and clear lower boundaries (cut-off) in the parallel direction. When the spacecraft moved closer to the separatrix, the cut-off velocity increased from ~200 km/s at 16:24:17 UT to ~400 km/s at 16:25:45 UT. The corresponding energies of these cut-off

velocities are marked with black triangles in Figure 2c, which are consistent with the ascending lower boundary in the parallel energy spectra of O^+ ions discussed above. Besides, the cold O^+ population might be heated and picked-up by the exhaust flow, thus showing ring distributions in Figures 2l and 2m, which is similar to the observations in Li et al. (2017) and Vines et al. (2017).

Fuselier et al. (2005) and Broll et al. (2017) studied several magnetopause reconnection events in which exhausting H^+ ions showed similar D-shaped velocity distributions. They also found that due to the conservation of the first adiabatic invariant, the cut-off of parallel velocity would become a curve in the v_{par} - v_{perp} plane if the exhausting ions move into a region with stronger magnetic fields. That is, the parallel velocity of exhausting ions would decrease if their initial v_{perp} is significant. Therefore, to get the accurate cut-off velocities, all the integrated v_{par} - v_{perp} plots of velocity distributions in this paper are shown in the reference frame where bulk $v_{perp} = 0$.

Based on the observations, it is clear that the spacecraft traveled from the central plasma sheet to the reconnection exhaust region, and then to the PSBL from 16:22 UT to 16:30 UT. The spacecraft trajectory is shown as the black dashed line in Figure 3.

3 Discussion

In this paper, we have reported that the lower boundary in the parallel direction can also be observed in the velocity distribution of O^+ ions in the magnetotail reconnection exhaust region. As mentioned above, Fuselier et al. (2005) studied the velocity distribution of H^+ ions in the magnetopause reconnection exhaust, which is characterized by the existence of similar cut-off in the parallel direction. Using a simple model that considers only exhausting H^+ ions, they suggested that the presence of this cut-off can be reasonably explained by the ToF effect, which can be understood by decomposing the velocity of the exhausting ions into the parallel and perpendicular (E×B drift) components. The magnitude and direction of the perpendicular drift velocity only depend on the local electromagnetic field configuration and do not depend on ion species or parallel velocity. Assuming that the reconnection process was in a steady-state, for those exhausting ions whose parallel velocity is smaller than the cut-off velocity mentioned above, their accumulated displacement in the perpendicular direction would be greater than the distance between the separatrix and spacecraft. Thus, they would not be observed by the spacecraft. The magnitude of this cut-off velocity depends on the position of the observation site in the exhaust region. The cut-off velocity will be the local deHoffman–Teller speed if the spacecraft is located very close to the neutral line. When the spacecraft moves towards the reconnection separatrix, the observed cut-off velocity will gradually increase to infinite.

The presence of the D-shaped distribution and cut-off velocity of O^+ ions in this event can also be explained by the ToF effect in the reconnection exhaust region described above. This provides direct evidence that the ionospheric O^+ ions can participate in the magnetotail reconnection processes. To compare the cut-off velocities of O^+ and H^+ ions, we plotted the integrated v_{par} - v_{perp} velocity distributions of O^+ and H^+ ions observed by SC4 at 16:27:03 UT (sampling time is 4 s), as shown in Figures 4a and 4b. The spacecraft was located close to the separatrix so that the

cut-off velocities were large enough to be identified clearly. The two plots share the same reference frame (v_{perpH} = 0) and axis range. The H^+ velocity distribution in Figure 4b is flipped upside down for comparison, and is part of the overall H^+ velocity distribution (Figure 4c) obtained from the CODIF data. It can be clearly seen from Figure 4 that the cut-off velocity of O^+ ions was about 400 km/s, apparently smaller than that of H^+ ions (~550 km/s) at the same time, as marked with black dashed lines.

It is worth to point out that this result is quite different from the theoretical model described by Fuselier et al. (2005) in which there should be no difference between the cut-off velocities of H^+ and O^+ ions. In their simplified model, it was assumed that the spacecraft was far from the reconnection diffusion region. That is, the spatial scale of the diffusion region could be neglected and all the exhausting ions could be regarded as departing from a single point. However, in our case, we believe that the spatial scale of the reconnection diffusion region and the width of the reconnection exhaust cannot be neglected. The ions departed from the edge of the diffusion region could travel a relatively shorter distance compared to the ions departed from the center of the diffusion region while accumulating the same displacement in the perpendicular direction to reach the observation site. Thus, their parallel velocities could be lower than those ions departed from the center of the diffusion region. It is reasonable to infer that the larger the diffusion region, the smaller will be the cut-off velocity. In our observations, O^+ ions have a lower cut-off velocity than H^+ ions, implying that O^+ ions have a larger diffusion region than H^+ ions. This agrees with the simulation results proposed by Liu et al. (2015) and Liang et al. (2017).

Next, we would like to further estimate the spatial scale ratio between O^+ and H^+ diffusion regions based on the above assumption. As shown in Figure 3, d_{sc} is the distance from the spacecraft to the center of the diffusion region in the X direction. The half widths of O^+ and H^+ diffusion regions are denoted by d_O and d_H, and the observed cut-off velocities are expressed as v_O and v_H, respectively. Assuming that the perpendicular velocities of O^+ and H^+ ions are the same in the exhaust region, the O^+ and H^+ ions having the corresponding cut-off parallel velocities can simultaneously reach the spacecraft after they departed from the edge of their diffusion regions. Their trajectories are sketched with red and blue lines in Figure 3.

The time taken by these O^+ and H^+ ions to move from the edge of their corresponding diffusion regions to the spacecraft are the same, and can be described as:

$$t = \frac{d_{sc} - d_H}{v_H} = \frac{d_{sc} - d_O}{v_O}$$

With the assumption that the spatial scale of the O^+ diffusion region is a times the H^+ diffusion region, we now have:

$$\frac{d_{sc}}{d_H} = \frac{a v_H - v_O}{v_H - v_O}$$

According to the observation, v_O is ~400 km/s and v_H is ~550 km/s in this event. Substituting these numbers in the above equation, we get:

$$\frac{d_{sc}}{d_H} \approx 5.5a - 4$$

For some magnetopause reconnection events, d_{sc} can be estimated pretty reliably using the Maximum Magnetic Shear model (Trattner et al., 2007a; Petrinec et al., 2016). However, it is usually difficult to determine the value of d_{sc} and d_H for the magnetotail reconnection events, unless the spacecraft happened to cross the reconnection separatrix or the neutral line (Xiao et al., 2007). For our event, we are unfortunately not able to further determine the value of d_{sc} and d_H. In addition, due to the limited energy resolution of the CODIF instrument, the values of v_O and v_H might be imprecise, as well. Nevertheless, the above formula can be treated as a remote-sensing method to estimate the spatial scale ratio between O^+ and H^+ diffusion regions and the distance from the spacecraft to the center of the reconnection region, when either of them is known.

4 Summary

In this study, we reported the D-shaped velocity distribution and the ToF effect of O^+ ions in the magnetotail reconnection exhaust, which can be treated as direct evidence that ionospheric O^+ ions can participate in the magnetotail reconnection process. The observed cut-off velocity of O^+ ions is smaller than that of H^+ ions at the same time, which is different from the previous theoretical prediction. We suggested that the difference between the two cut-off velocities is probably due to O^+ ions having a larger reconnection diffusion region than H^+ ions. We also demonstrated a remote-sensing method to estimate the spatial scale ratio between the O^+ and H^+ diffusion regions and the distance from the observation site to the center of the magnetotail reconnection region.

Acknowledgments

This work is supported by the National Nature Science Foundation of China (grants 41731068 and 41974191). We acknowledge the use of Cluster data from the ESA Cluster Active Science. The data can be found at CSA Archive: http://www.cosmos.esa.int/web/csa/. The Dst index data can be obtained from the World Data Center for Geomagnetism, Kyoto at http://wdc.kugi.kyoto-u.ac.jp/index.html. We thank E. Penou from CESR-Toulouse University/CNRS who developed the cl software for the data display.

References

Balogh, A., et al. (2001), The cluster magnetic field investigation: Overview of in-flight performance and initial results, Ann. Geophys., 19, 1207–1217, doi:10.5194/angeo-19-1207-2001.

Broll, J. M., Fuselier, S. A., and Trattner, K. J. (2017), Locating dayside magnetopause reconnection with exhaust ion distributions, J. Geophys. Res. Space Physics, 122, 5105– 5113, doi:10.1002/2016JA023590.

Eastman, T. E., Frank, L. A., Peterson, W. K., and Lennartsson, W. (1984), The plasma sheet boundary layer, J. Geophys. Res., 89(A3), 1553– 1572, doi:10.1029/JA089iA03p01553.

Eastwood, J. P., Phan, T. D., Øieroset, M., and Shay, M. A. (2010), Average properties of the magnetic reconnection ion diffusion region in the Earth's magnetotail: The 2001–2005 Cluster observations and comparison with simulations, J. Geophys. Res., 115, A08215, doi:10.1029/2009JA014962.

Echer, E., Korth, A., Zong, Q.-G., Fraünz, M., Gonzalez, W. D., Guarnieri, F. L., Fu, S. Y., and Reme, H. (2008), Cluster observations of O^+ escape in the magnetotail due to shock compression effects during the initial phase of the magnetic storm on 17 August 2001, J. Geophys. Res., 113, A05209, doi:10.1029/2007JA012624.

Fuselier, S. A., Trattner, K. J., Petrinec, S. M., Owen, C. J., and Rème, H. (2005), Computing the reconnection rate at the Earth's magnetopause using two spacecraft observations, J. Geophys. Res., 110, A06212, doi:10.1029/2004JA010805.

Fuselier, S. A., Burch, J. L., Mukherjee, J., Genestreti, K. J., Vines, S. K., Gomez, R., . . . Strangeway, R. J. (2017). Magnetospheric ion influence at the dayside magnetopause. Journal of Geophysical Research-Space Physics, 122(8), 8617-8631. doi:10.1002/2017ja024515

Fuselier, S. A., Trattner, K. J., Petrinec, S. M., Denton, M. H., Toledo-Redondo, S., Andre, M., . . . Strangeway, R. J. (2019). Mass Loading the Earth's Dayside Magnetopause Boundary Layer and Its Effect on Magnetic Reconnection. Geophysical Research Letters, 46(12), 6204-6213. doi:10.1029/2019gl082384

Johnstone, A.D., Alsop, C., Burge, S. et al. Space Science Reviews (1997) 79: 351. https://doi.org/10.1023/A:1004938001388.

Karimabadi, H., Roytershteyn, V., Mouikis, C. G., Kistler, L. M., & Daughton, W. (2011). Flushing effect in reconnection: Effects of minority species of oxygen ions. Planetary and Space Science, 59(7), 526-536. doi:10.1016/j.pss.2010.07.014

Kistler, L. M., et al. (2005), Contribution of nonadiabatic ions to the cross-tail current in an O^+dominated thin current sheet, J. Geophys. Res., 110, A06213, doi:10.1029/2004JA010653.

Kistler, L. M., et al. (2006), Ion composition and pressure changes in storm time and nonstorm substorms in the vicinity of the near-Earth neutral line, J. Geophys. Res., 111, A11222, doi:10.1029/2006JA011939.

Kronberg, E.A., Ashour-Abdalla, M., Dandouras, I. et al. (2014), Circulation of Heavy Ions and Their Dynamical Effects in the Magnetosphere: Recent Observations and Models, Space Sci Rev 184: 173. https://doi.org/10.1007/s11214-014-0104-0.

Lennartsson, W., and Shelley, E. G. (1986), Survey of 0.1- to 16-keV/e plasma sheet ion composition, J. Geophys. Res., 91(A3), 3061– 3076, doi:10.1029/JA091iA03p03061.

Li, W. Y., Andre, M., Khotyaintsev, Y. V., Vaivads, A., Fuselier, S. A., et al. (2017), Cold Ionospheric Ions in the Magnetic Reconnection Outflow Region. Journal of Geophysical Research-Space Physics, 122(10), 10194-10202. doi:10.1002/2017ja024287.

Liang, H., Ashour-Abdalla, M., Lapenta, G., and Walker, R. J. (2016), Oxygen impacts on dipolarization fronts and reconnection rate, J. Geophys. Res. Space Physics, 121, 1148– 1166, doi:10.1002/2015JA021747.

Liang, H., Lapenta, G., Walker, R. J., Schriver, D., El-Alaoui, M., and Berchem, J. (2017), Oxygen acceleration in magnetotail reconnection, J. Geophys. Res. Space Physics, 122, 618– 639, doi:10.1002/2016JA023060.

Liu, Y. H., Kistler, L. M., Mouikis, C. G., Klecker, B., & Dandouras, I. (2013). Heavy ion effects on substorm loading and unloading in the Earth's magnetotail. Journal of Geophysical Research-Space Physics, 118(5), 2101-2112. doi:10.1002/jgra.50240

Liu, Y. H., Kistler, L. M., Mouikis, C. G., Roytershteyn, V., and Karimabadi, H. (2014), The scale of the magnetotail reconnecting current sheet in the presence of O^+, Geophys. Res. Lett., 41, 4819– 4827, doi:10.1002/2014GL060440.

Liu, Y. H., Mouikis, C. G., Kistler, L. M., Wang, S., Roytershteyn, V., and Karimabadi, H. (2015), The heavy ion diffusion region in magnetic reconnection in the Earth's magnetotail. J. Geophys. Res. Space Physics,120, 3535– 3551. doi: 10.1002/2015JA020982.

Markidis, S., Lapenta, G., Bettarini, L., Goldman, M., Newman, D., and Andersson, L. (2011), Kinetic simulations of magnetic reconnection in presence of a background O^+ population, J. Geophys. Res., 116, A00K16, doi:10.1029/2011JA016429.

Mouikis, C. G., Kistler, L. M., Liu, Y. H., Klecker, B., Korth, A., and Dandouras, I. (2010), H^+ and O^+content of the plasma sheet at 15–19 Re as a function of geomagnetic and solar activity, J. Geophys. Res., 115, A00J16, doi:10.1029/2010JA015978.

Petrinec, S. M., Burch, J. L., Fuselier, S. A., Gomez, R. G., Lewis, et al. (2016), Comparison of Magnetospheric Multiscale ion jet signatures with predicted reconnection site locations at the magnetopause. Geophysical Research Letters, 43(12), 5997-6004. doi:10.1002/2016gl069626.

Phan, T. D., Sonnerup, B. U., and Lin, R. P. (2001), Fluid and kinetics signatures of reconnection at the dawn tail magnetopause: Wind observations, J. Geophys. Res., 106(A11), 25489– 25501, doi:10.1029/2001JA900054.

Rème, H., et al. (2001), First multispacecraft ion measurements in and near the Earth's magnetosphere with the identical Cluster Ion Spectrometry (CIS) experiment, Ann. Geophys., 19, 1303–1354, doi:10.5194/angeo-19-1303-2001.

Ruan, P., Fu, S. Y., Zong, Q.-G., Pu, Z. Y., Cao, X., Liu, W. L., Zhou, X. Z., and Daly, P. W. (2005), Ion composition variations in the plasma sheet observed by Cluster/RAPID, Geophys. Res. Lett., 32, L01105, doi:10.1029/2004GL021266.

Shay M A, Swisdak M. Three-Species collisionless reconnection: Effect of O^+ on magnetotail reconnection. Phys Rev Lett, 2004, 93, doi: 10.1103/PhysRevLett.93.175001

Shay, M. A., Drake, J. F., Denton, R. E., and Biskamp, D. (1998), Structure of the dissipation region during collisionless magnetic reconnection, J. Geophys. Res., 103(A5), 9165– 9176, doi:10.1029/97JA03528.

Sonnerup, B. U. Ö. (1979), Magnetic field reconnection, in Solar System Plasma Physics, vol. III, edited by E. N. Parker, C. F. Kennel, and L. J. Lanzerotti, pp. 45–108, Elsevier, New York.

Tenfjord, P., Hesse, M., Norgren, C., Spinnangr, S. F., & Kolstø, H. (2019), The impact of oxygen on the reconnection rate. Geophysical Research Letters, 46, 6195– 6203. https://doi.org/10.1029/2019GL082175.

Tenfjord, P., Hesse, M., & Norgren, C. (2018), The formation of an oxygen wave by magnetic reconnection. Journal of Geophysical Research: Space Physics, 123, 9370– 9380. https://doi.org/10.1029/2018JA026026.

Trattner, K. J., J. S. Mulcock, S. M. Petrinec, and S. A. Fuselier (2007a), Location of the reconnection line at the magnetopause during southward IMF conditions, Geophys. Res. Lett., 34, L03108, doi:10.1029/2006GL028397.

Vasyliunas, V. M. (1975), Theoretical models of magnetic field line merging, Rev. Geophys., 13(1), 303– 336, doi:10.1029/RG013i001p00303.

Vines, S. K., Fuselier, S. A., Trattner, K. J., Burch, J. L., Allen, et al. (2017), Magnetospheric Ion Evolution Across the Low-Latitude Boundary Layer Separatrix. Journal of Geophysical Research-Space Physics, 122(10), 10247-10262. doi:10.1002/2017ja024061.

Wang, S., Kistler, L. M., Mouikis, C. G., Liu, Y., and Genestreti, K. J. (2015), Hot magnetospheric O^+ and cold ion behavior in magnetopause reconnection: Cluster observations, J. Geophys. Res. Space Physics,119, 9601– 9623, doi:10.1002/2014JA020402.

Wilken, B., Zong, Q. G., Daglis, I. A., Doke, T., Livi, S., Maezawa, K., Pu, Z. Y., Ullaland, S., and Yamamoto, T. (1995), Tailward flowing energetic oxygen ion bursts associated with multiple flux ropes in the distant magnetotail: GEOTAIL observations. Geophys. Res. Lett., 22(23), 3267–327. https://doi.org/10.1029/95GL02980.

Wu, T., Fu, S. Y., Zong, Q. G., Sun, W. J., Cui, Y. B., Zhao, D., Guo, R. L., Zhao, S. J., and Wang, Y. F. (2016), Thin energetic O^+ layer embedded in the magnetotail reconnection current sheet observed by Cluster, Geophys. Res. Lett., 43, 11,493– 11,500, doi:10.1002/2016GL071184.

Xiao, C. J., Pu, Z. Y., Wang, X. G., Ma, Z. W., Fu, S. Y., et al. (2007), A Cluster measurement of fast magnetic reconnection in the magnetotail. Geophysical Research Letters, 34(1). doi:10.1029/2006gl028006

Yue, C., Bortnik, J., Li, W., Ma, Q., Wang, C.-P., Thorne, R. M., et al (2019), Oxygen Ion Dynamics in the Earth's Ring Current: Van Allen Probes Observations. Journal of Geophysical Research: Space Physics, 124. https://doi.org/10.1029/2019JA026801

Yue, C., Bortnik, J., Li, W., Ma, Q., Gkioulidou, M., Reeves, G. D., et al. (2018), The composition of plasma inside geostationary orbit based on Van Allen Probes observations. Journal of Geophysical Research: Space Physics, 123, 6478–6493. https://doi.org/10.1029/2018JA025344

Zhao, S. J., Fu, S. Y., Sun, W. J., Parks, G. K., Zhou, X. Z., Pu, Z. Y., et al. (2018). Oxygen ion reflection at earthward propagating dipolarization fronts in the Magnetotail. Journal of Geophysical Research: Space Physics, 123, 6277– 6288. https://doi.org/10.1029/2018JA025689.

Zong, Q.-G., et al. (1997), Geotail observations of energetic ion species and magnetic field in plasmoid-like structures in the course of an isolated substorm event, J. Geophys. Res., 102(A6), 11409– 11428, doi:10.1029/97JA00076.

Zong, Q. G., et al. (2004), Cluster observations of earthward flowing plasmoid in the tail. Geophysical Research Letters, 31(18). doi:10.1029/2004gl020692

Zong, Q.-G., Zhang, H., Fu, S. Y., Wang, Y. F., Pu, Z. Y., Korth, A., Daly, P. W., and Fritz, T. A. (2008), Ionospheric oxygen ions dominant bursty bulk flows: Cluster and Double Star observations, J. Geophys. Res., 113, A07S23, doi:10.1029/2007JA012764.

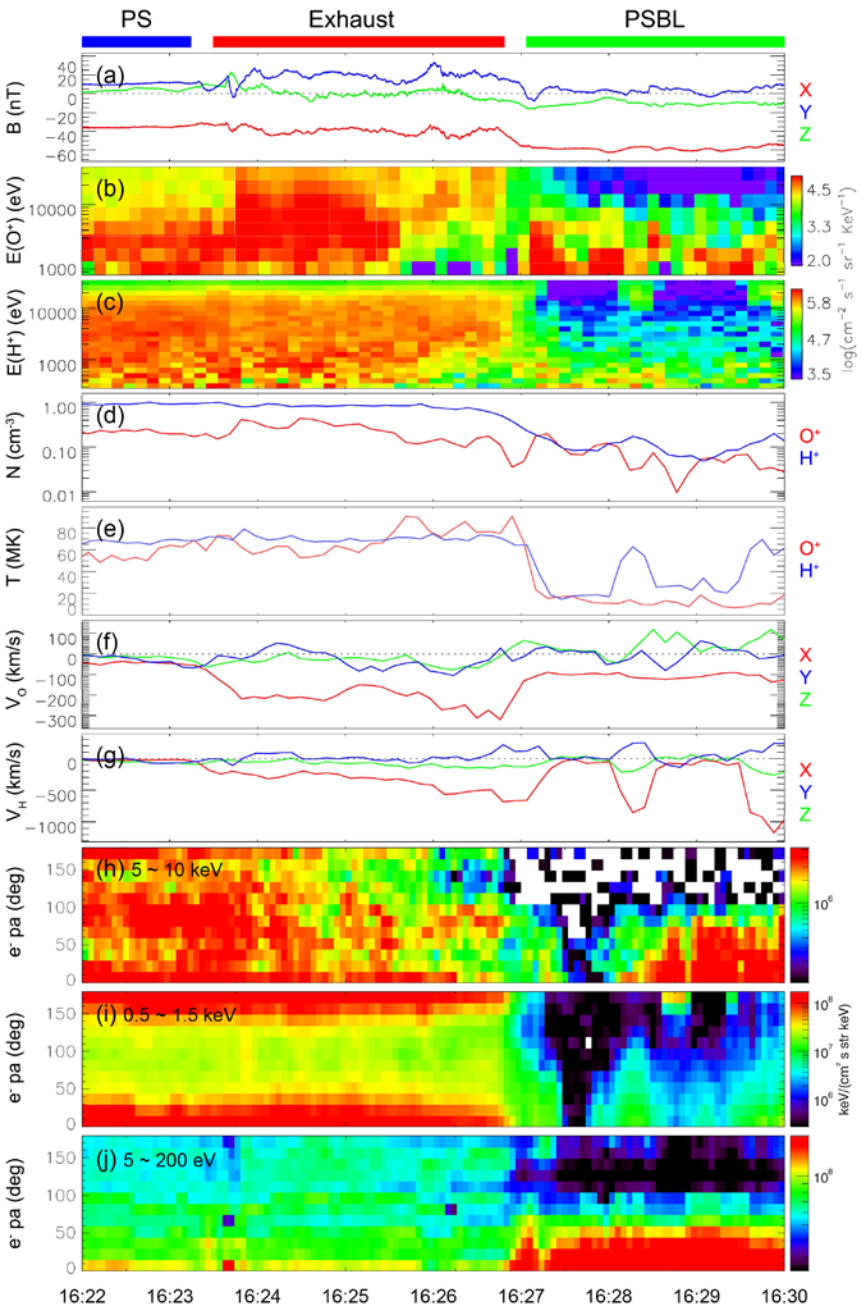

Figure 1. (**a**) Magnetic field components observed by SC1 during 16:22 UT to 16:30 UT, similarly hereinafter. Red, blue, and green lines represent Bx, By, and Bz, respectively. (**b**) and (**c**) Differential particle fluxes of O^+ and H^+, respectively. (**d**) and (**e**) Number densities and

temperatures of O^+ (red line) and H^+ (blue line), respectively. (**f**) and (**g**) Bulk velocity components of O^+ (red line) and H^+ (blue line), respectively. (**h**) ~ (**j**) Pitch angle distributions of electrons with different energy ranges. (5–10 keV; 0.5–1.5 keV and 5–200 eV). Different regions (central plasma sheet, reconnection exhaust region, and plasma sheet boundary layer) are marked with blue, red and green bars at the top of panel (a), respectively.

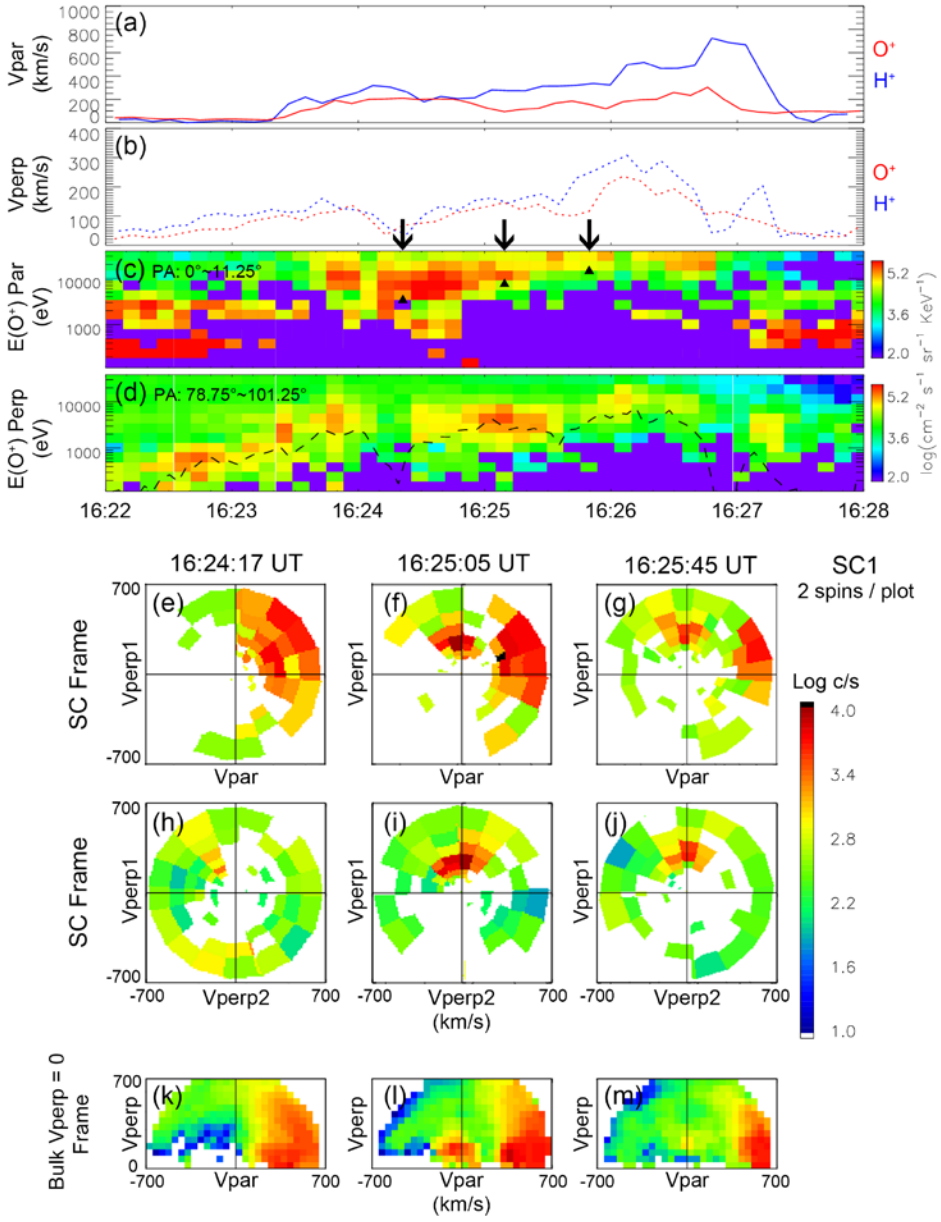

Figure 2. (**a**) and (**b**) Parallel and perpendicular velocities of O^+ (red line) and H^+ (blue line) ions. (**c**) and (**d**) Differential particle flux of O^+ ions in parallel and perpendicular directions. The dashed line in panel (d) shows the estimated O^+ characteristic energy derived from HIA ion perpendicular velocity data. (**e**) ~ (**j**) v_{par} - v_{perp1} and v_{perp2} - v_{perp1} slices of O^+ velocity distributions. (**k**) ~ (**m**) integrated v_{par} - v_{perp} O^+ velocity distributions in the bulk v_{perp} = 0

reference frame. The observation time of each column in (e) ~ (m) is marked with black arrow above panel (c).

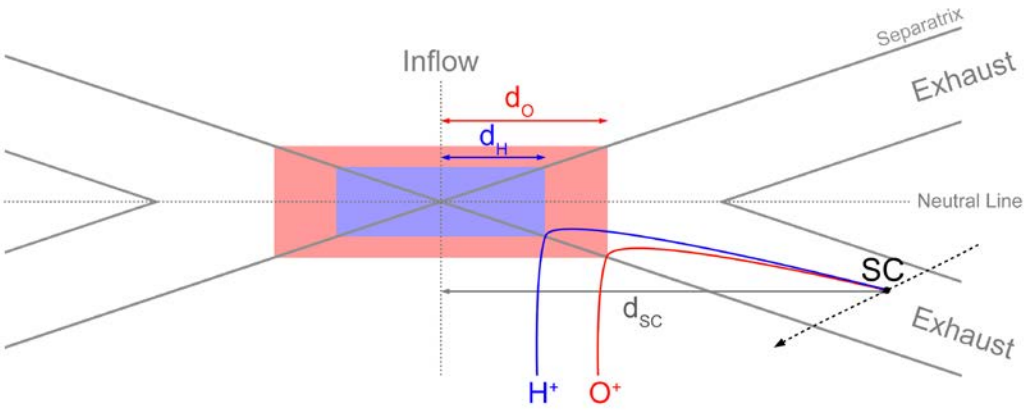

Figure 3. Schematic plot of the spacecraft trajectory from 16:22 UT to 16:30 UT relative to the reconnection region. Red and blue lines show the trajectories of O^+ and H^+ ions with their corresponding cut-off velocity that are observed by the spacecraft. See text for details.

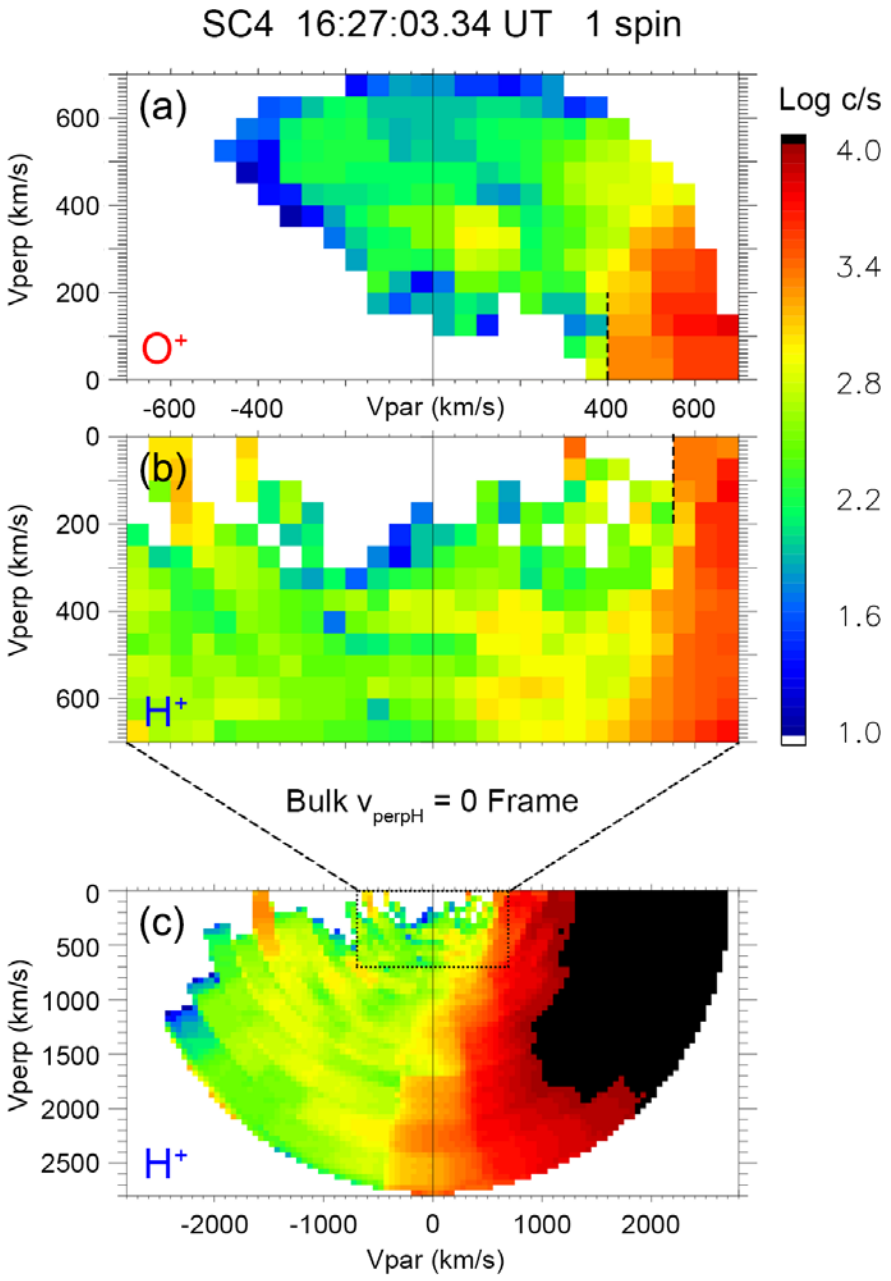

Figure 4. (**a**) and (**b**) integrated v_{par} - v_{perp} velocity distributions of O^+ and H^+ ions observed by SC4 at 16:27:03 UT. H^+ velocity distribution is flipped upside down for comparison. (**c**) Overall H^+ velocity distribution.

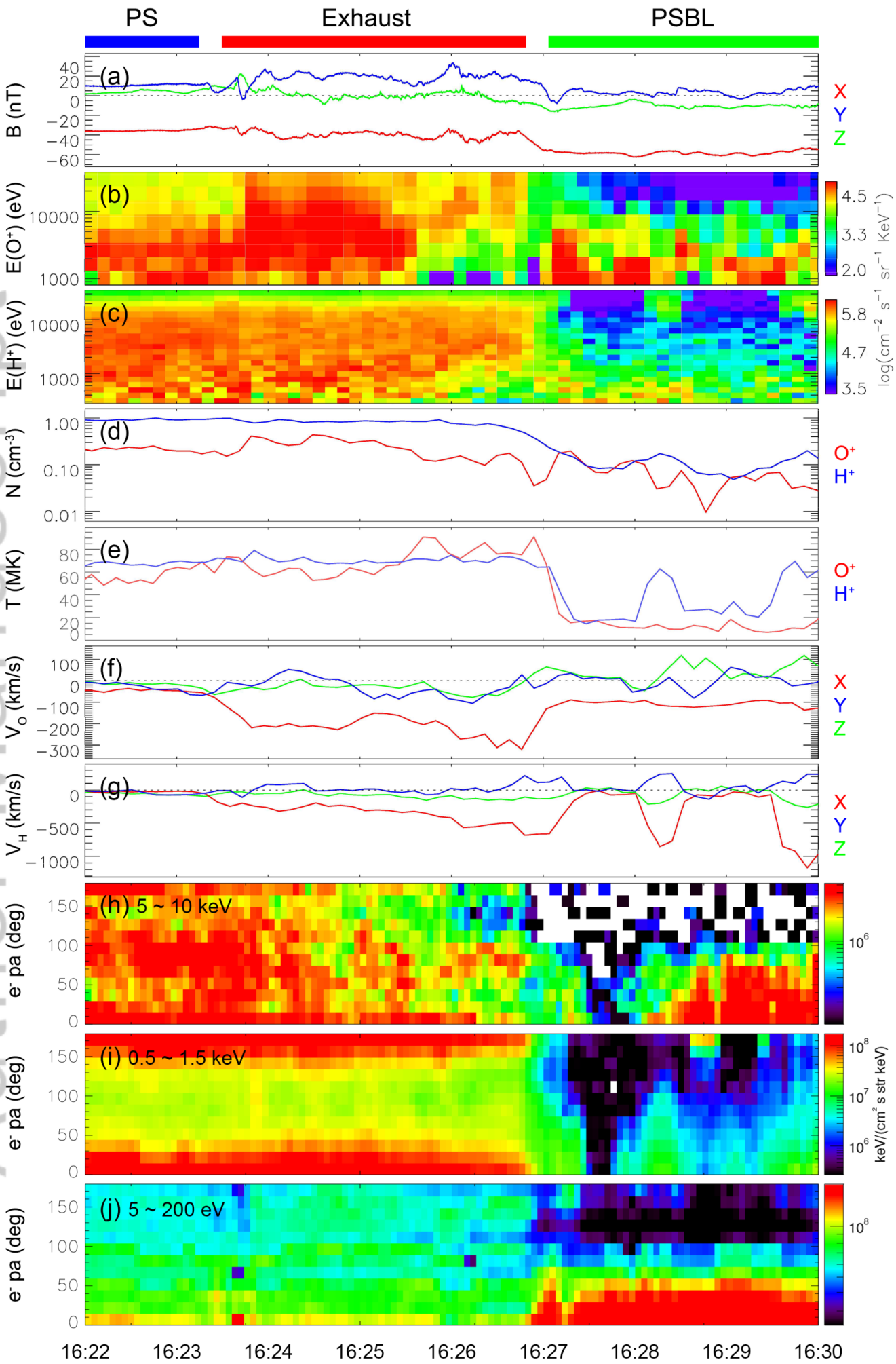

2019GL085200-f01-z-.png

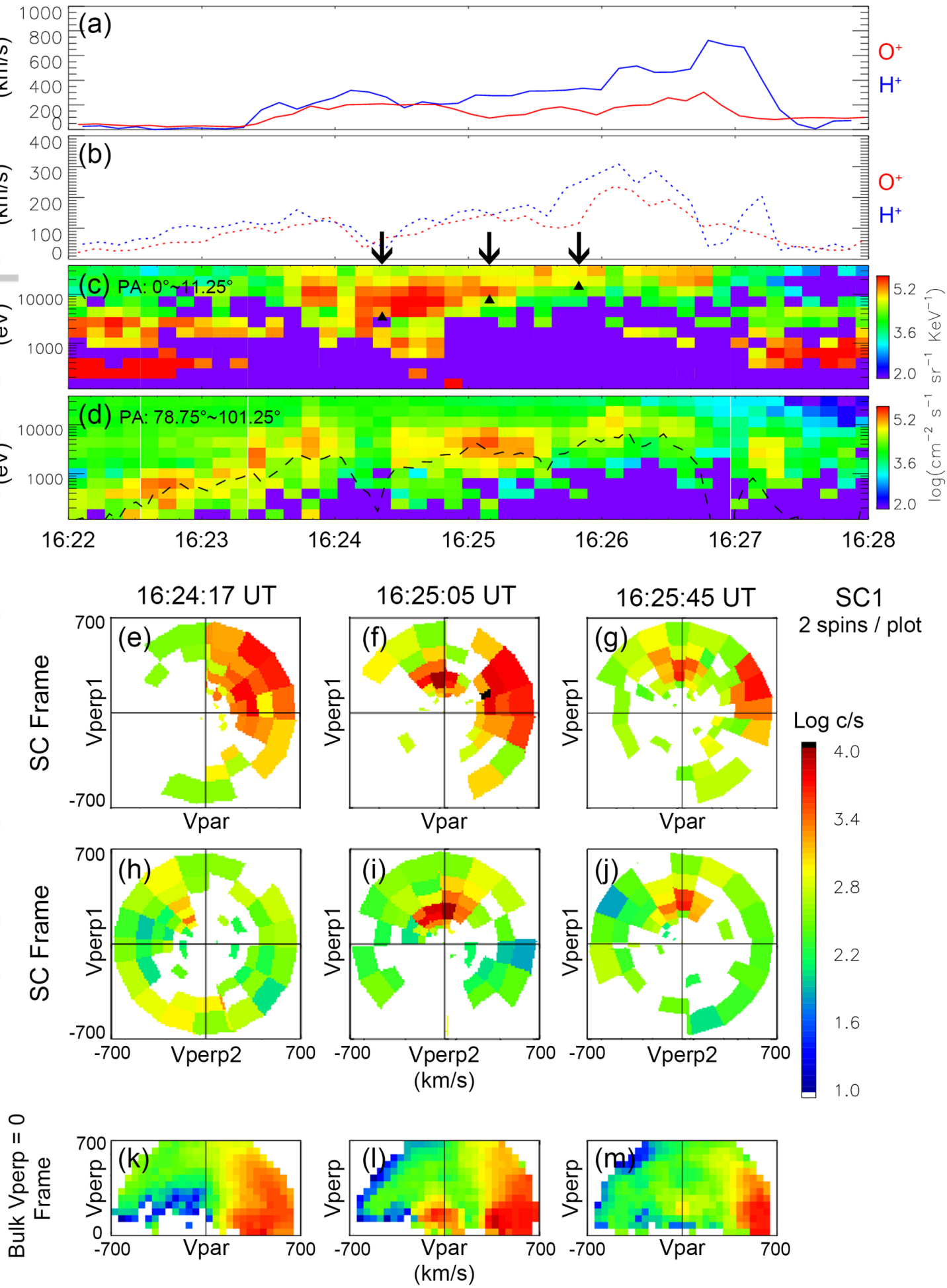

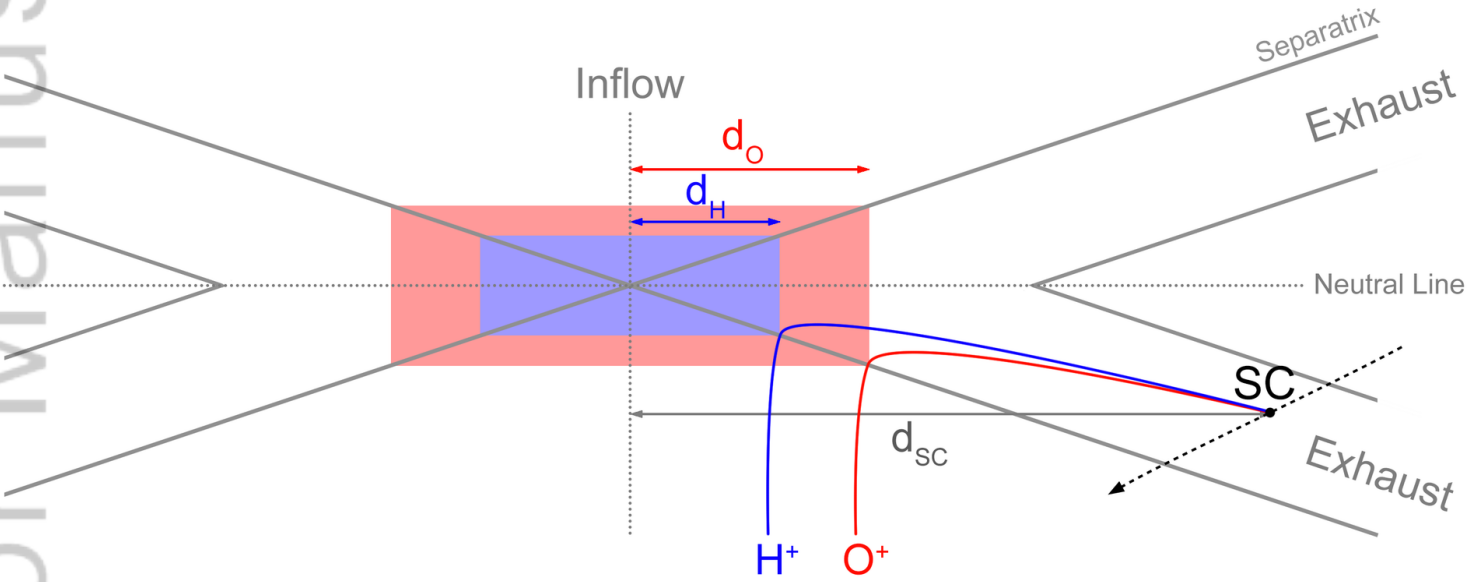

2019GL085200-f03-z-.png